Design and Characterization of an Aerostatic Spherical Bearing

Alec P. Robertson*, Alexander H. Slocum
Department of Mechanical Engineering
Massachusetts Institute of Technology
Cambridge, MA 02139, USA

Abstract

An aerostatic spherical bearing has been developed for parallel kinematic machines. The design is based on a ball and socket configuration and is preloaded by permanent magnets arranged about the socket. High pressure air is injected through three orifices into the cavity between the ball and socket to produce a low friction, high accuracy interface. Joint accuracy is measured using a coordinate measurement machine and found to be 16 μm throughout the joint working range; this can be reduced to 11 μm through calibration of the joint error parameters. The flow properties are modeled using a Navier-Stokes flat-plate approximation and agree with measurements to 10 % within the joint operating range.

1 Introduction

Aerostatic bearings are commonly used in high accuracy applications such as coordinate measurement machines (CMM) and high-speed spindles. Porous materials or discrete orifices are typically used to introduce compressed air into the region between two precision surfaces. For small air gaps, this produces a stable fluidic layer with significantly lower friction than sliding lubricated surfaces. The most common examples of aerostatic bearings are rectangular or circular flat plate bearings that are used to support the linear stages on a CMM; and cylindrical bearings used to support spindle shafts for high speed machining centers [1]. Spherical aerostatic bearings offer opportunities for motion in three dimensions, namely rotary motion about each of the joint's x-, y- and z-axes. A ball and socket configuration represents a high precision design for a spherical joint, as all three axes are co-located [2]. This reduces the errors inherent in kinematic three degree-of-freedom structures such as modified universal joints, or other mechanical configurations [3].

This paper describes the development and testing of a three degree of freedom aerostatic bearing. Section 2 describes the design and construction of the bearing and Section 3 models its accuracy and fluid flow properties. Finally, in Section 4 the models are compared with measured data from the joint prototype.

*Corresponding author: alecr@mit.edu

2 Design Process

The aerostatic joint is required to have a singularity-free working range of 180° and an accuracy of several micrometers. The joint prototype has an aluminum socket turned from 90 mm cylindrical stock (alloy 6061) and a 50 mm diameter (grade 50) solid steel ball bearing. A magnetic preload between the ball and socket is provided by eight 12 mm diameter magnets in a single ring around the socket.

An accurate mounting surface between the ball and the socket is created through replication with a Teflon-laced epoxy [4]. The ball is coated with a wax compound to achieve an even surface layer for a nominal initial air gap height of approximately 10 μm. Additionally, a mold release is applied to the wax coating to facilitate removal of the ball following replication. The resultant surface finish may be rougher than for direct replication of a steel surface because of the wax compound; furthermore, plastic deformation of the wax due to the high contact forces at the orifices may cause slight indentations in the replicated surface. These irregularities can be removed with fine grit sandpaper. High-pressure air is then injected into the base of the socket via three 50 μm diameter ruby orifices [5], creating an air gap that supports the ball.

The replicated socket is shown in Figure 1 and the

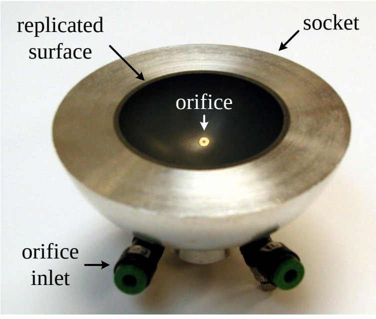

Figure 1: Fluid contact socket.

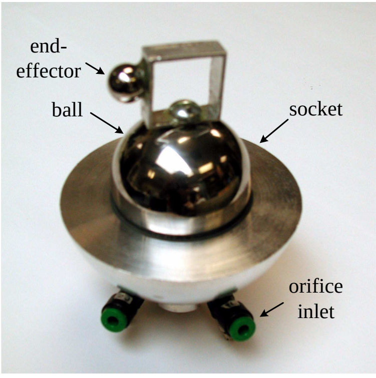

Figure 2: Fluid contact joint.

complete joint with ball and end-effector is shown in Figure 2.

3 Modeling

3.1 Accuracy Model

Measurement and calibration of the joint's positional accuracy is achieved using calibration techniques developed for industrial manipulators [6]. The modeling of the ball and socket joint is presented elsewhere; measurements of similar joint prototypes based on a rolling contact mechanism show a positional accuracy of 12 μm uncalibrated and 8 μm calibrated [7]. Using a Monte Carlo analysis [8], the aerostatic joint accuracy is predicted to be 11 μm by considering errors such as ball asphericity and replication errors.

3.2 Fluid Model

A simplified Navier-Stokes representation is used to model the fluid flow characteristics. Due to the high aspect ratio between joint surface area (several square centimeters) and air gap (tens of micrometers), the joint is approximated by two parallel flat plates. Given the orifice specifications – pressure drop

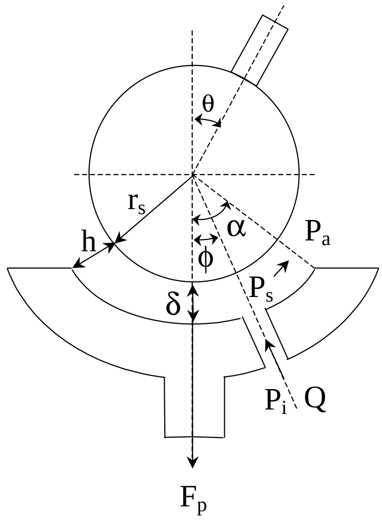

Figure 3: Socket flow schematic. Note that the schematic is not to scale and $r_s \gg h$.

versus flow rate characteristics – the inlet pressure can be expressed as a function of the air gap. Measurement of the air gap versus inlet pressure is then used to validate the flat-plate approximation.

The maximum preload force for the aerostatic joint is measured to be 90 N for the single row of magnets. The volume flow rate and pressure required to create an air gap under this preload force needs to be determined for a given orifice aperture diameter. The pressure and flow schematic is shown in Figure 3, where the orifice air supply enters at gauge pressure P_i and flow rate Q, at an angle ϕ from the vertical and exits at the socket edge (angle α) with atmospheric pressure P_a. The flow rate is constant through the air gap due to the assumption of incompressible flow. The pressure drop P_s along the socket supports the ball, hence the total vertical component of the pressure force must support the bearing against the magnetic preload force F_p. This is modeled as the ratio of the preload force to the projected socket area:

$$P_s = \frac{F_p}{\pi \left(r_s \sin \alpha\right)^2} \quad (1)$$

The Navier-Stokes equation in the radial direction can be simplified and solved to determine the pressure drop across the orifices:

$$P_o = \frac{6 \mu P_s R_o}{\pi h^3 N_o} \ln \left(\frac{l_s}{l_o}\right) \quad (2)$$

Where the socket arc length l_s is the distance swept by the socket angle, scaled by the plate-sphere radius ratio η:

$$l_o = \eta \, r_s \, \alpha \quad (3)$$

The orifice arc length l_o is calculated in a similar fashion. The scaling factor η is determined by equating the surface area of a sphere of arc angle α and radius r_s $\left(\frac{\alpha}{\pi} \cdot 4\,\pi\, r_s^2\right)$, to the equivalent area of a flat-plate of radius r_p $\left(\pi\, r_p^2\right)$, leading to the relationship:

$$\eta = \frac{r_p}{r_s} = \sqrt{\frac{4\,\alpha}{\pi}} \quad (4)$$

The resistance of the orifice R_o is supplied by the manufacturer, N_o is the number of orifices used and μ is the viscosity of air. The inlet gauge pressure P_i is the sum of the socket and orifice pressure drops:

$$P_i = P_s + P_o \quad (5)$$

The socket outlet is believed to act as a restrictor for the fluidic system. The air gap h is therefore assumed to be the separation of ball and socket at the socket edge and is geometrically related to the vertical displacement δ:

$$h = \delta \, cos \, \alpha \quad (6)$$

For socket angles approaching 90° this relationship degrades and an average air gap should be calculated using the cubic weighted average of the gap heights along the socket. The relationship between the inlet pressure P_i and the vertical displacement δ is compared to measured data in Section 3.2 to validate this simplified Navier-Stokes approach.

4 Measurements

4.1 Accuracy Measurements

The maximum and mean errors for the aerostatic joint are shown are Figure 4, showing a maximum uncalibrated (geometric) error of $16\,\mu m$ and a calibrated (kinematic) error of $11\,\mu m$. This compares favorably with the predicted accuracy of $11\,\mu m$. The large maximum error is believed to be due to slight inaccuracies in the replication process. The uncalibrated mean error is found to be $4\,\mu m$ which renders this joint suitable for high accuracy robotic applications.

4.2 Fluid Measurements

A coordinate measurement machine accurate to $2\,\mu m$ is used to measure the displacement of the ball center as the inlet gauge pressure is increased from 0 to $7 atm$ as shown in Figure 5. For inlet pressures above $3\,atm$,

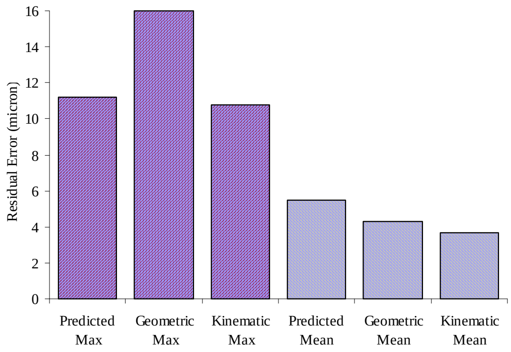

Figure 4: Comparison of joint accuracy.

corresponding to an air gap of about $20\,\mu m$, the measured and predicted vertical displacements agree to within 10 %. However, at lower pressures the model underestimates the displacement and is accurate only to 15 %, believed to be due to surface irregularities affecting fluid flow at small gap sizes. For inlet pressures greater than $7\,atm$ pneumatic hammer is observed, which is a common occurrence for large air gaps [9]. Therefore, for a desired operating pressure range of 3 to $7\,atm$, the flat-plate Navier Stokes model represents a suitable first order approximation.

To improve the correlation between predicted and measured displacements the Navier Stokes in spherical coordinates could be used. Alternatively, the outlet gap size h could be directly measured with capacitance probes and compared to the predicted. The volume flow rate Q can also be measured with a flow meter and compared to the predicted flow rate.

5 Conclusion

The spherical aerostatic contact joint is approximated by a first order flat plate model in order to predict the pressure versus displacement characteristics. Within the inlet pressure operating region of 3 to $7\,atm$, corresponding to an operating air gap of $20\,\mu m$, the model agrees with measurements to within 10 %. This is sufficient to allow first order predictions of the aerostatic contact joint performance. The agreement between measured and predicted vertical displacements for pressures below $3\,atm$ is only to within 15 %, assumed to be due to the poor replication surface finish. Direct replication of the ball could improve the surface finish and consequently the low-pressure performance.

The joint accuracy maximum error is $16\,\mu m$ uncalibrated and $11\,\mu m$ when calibrated. This is slightly higher than predicted, due to the inaccuracies inher-

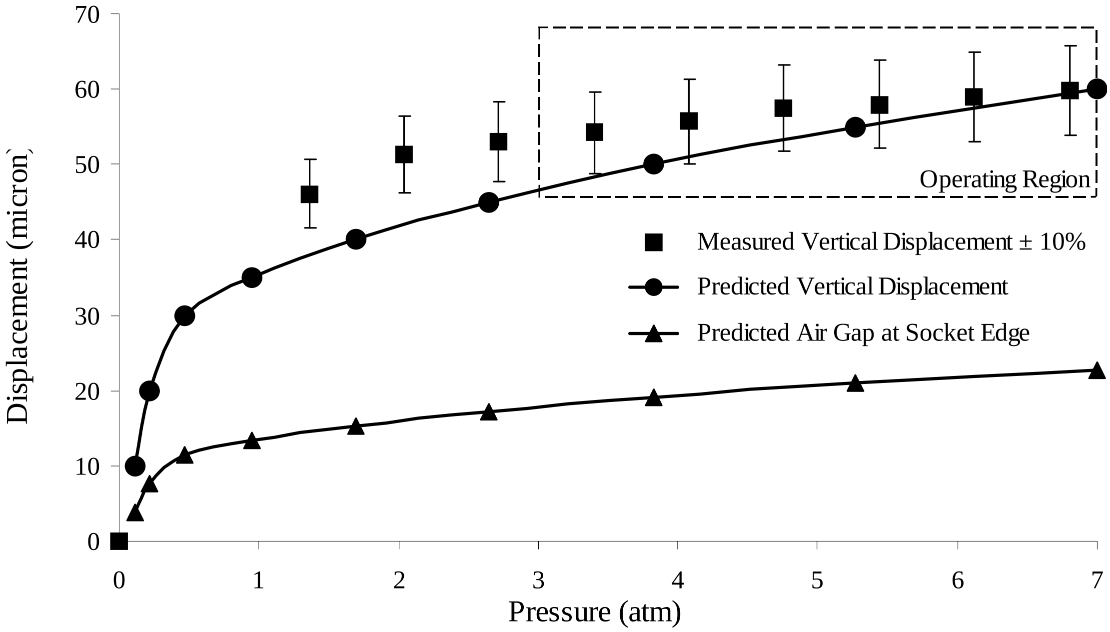

Figure 5: Pressure-displacement characteristics for aerostatic contact joint. The predicted and measured vertical displacements agree to within 10 % for the inlet pressure operating region of 3 to 7 atm.

ent in the replication process. Improved control of the replication process and resultant surface finish should result in a smaller operating gap and an improved overall accuracy.

Additional work is required to characterize the joint stiffness and damping. Preliminary tests indicate that the aerostatic joint stiffness is approximately $5\,N/\mu m$ which agrees to within 10 % with the predicted stiffness from the Navier Stokes flat-plate model. Damping is noticeable in the aerostatic joint, believed to be due to the viscosity of air in a small gap and hysteresis from induced magnetic fields in the ball. Characterization of the joint damping and stiffness would allow a simple spring-mass-damper model to be developed and the dynamic performance evaluated.

6 Acknowledgements

The authors would like to thank ABB for their support during this research.

References

[1] A. H. Slocum, Precision Machine Design, Society of Manufacturing Engineers, Michigan, 1992, Ch. 9.3, pp. 580–625.

[2] J. B. Bryan, Telescoping magnetic ball bar test gage, US Patent #4,435,905.

[3] L. F. Bieg, G. L. Benavides, Double slotted socket spherical joint, US Patent #6,234,703.

[4] Moglice, Moglice replication fluid (2003). URL `http://www.moglice.com/`

[5] Bird Precision, Bird precision orifices (2003). URL `http://www.birdprecision.com/`

[6] R. Bernhardt, S. Albright, Robot Calibration, Chapman and Hall, London, 1993.

[7] A. Robertson, A. Rzepniewski, A. Slocum, Measurement and calibration of high accuracy spherical joints, in: A. S. for Precision Engineering (Ed.), Proceedings ASPE 2002 Annual Meeting, 2002, pp. 223–227.

[8] D. D. Frey, K. N. Otto, W. Pflager, Swept envelopes of cutting tools in integrated machine and workpiece error budgeting, Annals of the CIRP 46 (1997) 475–480.

[9] H. M. Talukder, T. B. Stowell, Pneumatic hammer in an externally pressurized orifice-compensated air journal bearing, Tribology International 36 (8) (2003) 585–591.

Keywords: aerostatic bearing, spherical joint, parallel kinematic machines